RESEARCH ARTICLE

CrossMark

Water decontamination containing nitrate using biosorption with *Moringa oleifera* in dynamic mode

Rebecca Manesco Paixão[1] · Isabela Maria Reck[2] · Raquel Guttierres Gomes[3] · Rosângela Bergamasco[1] ·
Marcelo Fernandes Vieira[1] · Angélica Marquetotti Salcedo Vieira[3]

Abstract
This study was conducted to assess the feasibility of using *Moringa oleifera* Lam. (MO) seeds in the biosorption of nitrate present in aqueous solutions by means of batch and fixed-bed column biosorption processes. The batch assays showed that nitrate biosorption is enhanced under experimental conditions of pH 3 and a biosorbent mass of 0.05 g. For the experiments in dynamic mode, the results obtained from the statistical parameters showed that lesser pH, lesser feed flow rate, and higher initial concentration will result in an increase of the maximum capacity of the bed. These conditions were confirmed by experimental analysis. The best experimental conditions, according to the values for percentage removal (91.09%) and maximum capacity (7.69 mg g^{-1}) of the bed, were those used in assay 1, which utilized pH 3, feed flow rate of 1 mL min^{-1}, and initial nitrate concentration of 100 mg L^{-1}.

Introduction

Nitrate is a water contaminant widespread in the world, due to its stability, high water solubility, and lack of awareness of the population (Jain et al. 2015). Nitrogen in the biochemical process of conversion of ammonia to nitrite, and this to nitrate, may lead to the consumption of dissolved oxygen in the environment, affecting aquatic life. Also, nitrogen in the form of nitrate present in drinking water can cause diseases such as cancer and methemoglobinemia; also, studies indicate that it can cause diabetes and hypertension and increase blood pressure (Weyer et al. 2001; Galloway et al. 2003; Aghaii et al. 2013; Eneji

et al. 2013; Jain et al. 2015; Golie and Upadhyayula 2016). Thus, the World Health Organization set a limit of 50 mg L^{-1} as the maximum allowable concentration of nitrate in drinking water (WHO 2011).

In this context, various techniques for nitrate removal have been studied, such as ion exchange, reverse osmosis, and chemical and biological reduction (Ota et al. 2013), but among these, adsorption seems to be the most attractive technique in terms of cost, simplicity of design and operation, regenerative capacity, and reduction/minimization of different types of organic and inorganic pollutants in water and wastewater (Bhatnagar and Sillanpää 2011; Jain et al. 2015). The adsorption process can be carried out by batch or in a fixed-bed column; and processes for large-scale adsorption in a fixed-bed column are the most used, because they are more efficient for treating large volumes of effluents and in adsorption/desorption cycles, since they make more efficient use of the adsorbent capacity, resulting in better effluent quality. Besides, they have other advantages, such as high-yield operations and easy transportation at laboratory scale (do Nascimento et al. 2014; Golie and Upadhyayula 2016).

Biosorption is the ability of biological materials to remove pollutants from water, and biosorbents are used worldwide due to their natural environment availability,

✉ Angélica Marquetotti Salcedo Vieira
amsvieira@uem.br

[1] Chemical Engineering Department, State University of Maringa, Av Colombo, Maringa, Parana 5790, Brazil

[2] Postgraduate Program in Food Science, State University of Maringa, Av Colombo, Maringa, Parana 5790, Brazil

[3] Food Engineering Department, State University of Maringa, Av Colombo, Maringa, Parana 5790, Brazil

low cost, and biodegradability (Farrokhzadeh et al. 2013; Matouq et al. 2015). *Moringa oleifera* Lam. (MO) is a plant of north-eastern India, easily cultivable in tropical and subtropical regions, which has nutritional, medicinal, and water-cleaning attributes (Reddy et al. 2011), being used mainly in coagulation processes, clarification, and adsorption of pollutants in aqueous solutions (Meneghel et al. 2013; Baptista et al. 2015). Its seeds, in particular, are regarded as a natural coagulant, having cationic proteins responsible for clarifying turbid water (Gopalakrishnan et al. 2016; Baptista et al. 2017). Aqueous and saline extracts of MO seeds have been used in the coagulation of water for public supply, in order to remove color, turbidity, organic matter, and dissolved organic carbon, with good results obtained (Baptista et al. 2015, 2017; Rezende et al. 2016). Despite the studies that prove the efficiency of MO seeds for the removal of several surface water and groundwater contaminants, few studies have shown its application in dynamic processes. Confirmation of MO application capability could broaden the field of research and use of this biosorbent. Thus, the purpose of this study was to remove nitrate from aqueous solutions, using the seeds of *Moringa oleifera* Lam. as a biosorbent in batch and fixed-bed column biosorption processes.

Materials and methods

Biosorbent preparation

The fresh fruits of *Moringa oleifera* Lam. were obtained in Aracaju, Sergipe, Brazil. To prepare the biosorbent, first, the parts of the MO, bark and seeds, were separated manually. The seeds were ground and homogenized in a processor, washed with deionized water to remove color, dried in an oven with air circulation at 40 °C until constant weight was achieved (Amagloh and Benang 2009), and finally sieved through an 0.8-mm Bertel screen pack.

Biosorbent characterization

The point of zero charge (pH_{PZC}) is defined as the pH at which the surface of a biosorbent has neutral overall charge. Its determination was performed according to "trial of 11 points" methodology (Regalbuto and Robles 2004).

To evaluate the morphological characteristics of the biosorbent, scanning electron microscopy (SEM) using an SEM SS 550 Superscan (Shimadzu) was carried out. The analysis of functional groups was carried out by Fourier transform infrared spectroscopy (FTIR) before and after the biosorption of nitrate using a Bomen FTIR Spectrometer with 21 scans 100 min^{-1} and a resolution of 4 cm^{-1}.

Preparation and determination of nitrate solution

A synthetic solution of nitrate (NO_3^-) was prepared from a stock solution of 100 mg L^{-1} $NaNO_3$ diluted in deionized water, and its determination was performed on a spectrophotometer at 205 nm as proposed by IAL (2008).

Batch biosorption assays

The batch biosorption study was performed in a cooled incubator, setting the experimental conditions at room temperature (25 °C ± 1), biosorbent mass of 0.2 g, 100 rpm rotation, unadjusted pH (5.0 ± 0.2), and initial nitrate concentration of 100 mg L^{-1}. The following parameters were evaluated: contact time (10–600 min), pH (2–10), and adsorbent mass (0.05–1.5 g), as well as desorption, in order to evaluate the regeneration and reuse of the biosorbent. After the equilibrium time, samples were filtered through 0.45-μm Millipore membranes and the nitrate concentration determined by spectrophotometer. All assays were conducted in doubles and the results expressed as the average result.

The amount of nitrate adsorbed (q_e) was calculated according to Eq. 1, while the nitrate desorption percentage (q_{ds}) was calculated according to Eq. 2:

$$q_e = \frac{(C_i - C_e)}{m} \cdot V \tag{1}$$

$$q_{ds} = \frac{(C_{ds} \cdot V)}{m} \tag{2}$$

where q_e is the amount of nitrate adsorbed at equilibrium (mg g^{-1}), V is the nitrate solution volume (L), C_i is the initial nitrate concentration in solution (mg L^{-1}), C_e is the nitrate concentration at equilibrium (mg L^{-1}), m is the mass of biosorbent (g), q_{ds} is the amount of desorbed nitrate at equilibrium (mg g^{-1}), and C_{ds} is the desorbed nitrate concentration (mg L^{-1}).

Fixed-bed column biosorption assays

One of the most important factors in measuring the feasibility of a biosorbent in real and practical application is the performance of biosorption process in a continuous fixed-bed column. In fact, the results from batch studies only present the biosorption equilibrium and kinetics (Shanmugaprakash and Sivakumar 2015). Therefore, in order to predict the performance of MO to remove nitrate, experiments were carried out in a dynamic mode.

In the fixed-bed column biosorption study, the following parameters were evaluated: initial concentration (50, 75, and 100 mg L^{-1}), solution pH (3.0, 5.5, 7.0) and feed flow rate (1, 3, and 5 mL min^{-1}). Therefore, breakthrough curves were

constructed using an experimental factorial design with three levels (2^3) and four central points.

The pH values were chosen as a function of the higher adsorption capacity, determined in the batch tests. The initial concentration and flow rate were chosen based on the literature.

The assays were conducted in a glass column of 28 cm height and 0.9 cm internal diameter, positioned vertically so that the biosorbent was packaged according to the "slurry method" (Zach-Maor et al. 2011) using 1.0 g of MO seeds moistened with deionized water (equivalent to a height of 2.5 cm) at room temperature (25 °C ± 1). The water contaminated with nitrate (NO_3^-) was fed to the bed in upflow by a Masterflex peristaltic pump, and the effluent samples were collected at established time intervals until saturation of the bed, when $C_t/C_0 = 0.9$.

The total solute capacity in the fixed-bed for a given concentration and flow rate may be obtained by calculating the area below the breakthrough curve (Paudyal et al. 2013) given by Eq. 3:

$$q_t = \frac{Q.A}{1000} = \frac{Q}{100} \int_{t=0}^{t=t_{total}} C_{ad}.dt \qquad (3)$$

where q_t is the amount of solute adsorbed on the bed (mg), Q is the volumetric feed flow (mL min^{-1}), A is the area below the breakthrough curve, C_{ad} is the adsorbed concentration on the bed (mg L^{-1}), and t is the total feed time (min), which could be t_{total}, t_s or t_r that represent the total flow time, the saturation or exhaustion time ($C_t/C_0 = 0.90$), or the breakthrough time ($C_t/C_0 = 0.10$), respectively.

The adsorbed concentration in the bed, C_{ad}, can be obtained by calculating the difference between the feed concentration (C_0) and the outlet concentration (C_t) of the bed as given by Eq. 4:

$$C_{ad} = C_0 - C_t \qquad (4)$$

The maximum capacity of the bed (q_e) is calculated by the total amount of solute adsorbed (q_t) per mass of adsorbent (m) (Nguyen et al. 2015), according to Eq. 5:

$$q_e = qt/m \qquad (5)$$

The total amount of adsorbate sent to the bed at the end of feeding time (W_t) is calculated by Eq. 6:

$$W_t = \frac{C_0.Q.t_s}{1000} \qquad (6)$$

Where C_0 is the feed concentration (mg L^{-1}), Q is the feed flow rate (mL min^{-1}) and t_s is the bed saturation time (min).

The calculation of the total percentage removal (Y), presented in Eq. 7, can be done by relating the total amount of adsorbate sent to the bed at the end of feeding time (W_t) with the amount of solute adsorbed on the bed (q_t):

$$Y = \frac{q_t}{W_t}.100 \qquad (7)$$

For experimental design, the maximum capacity of the bed (q_e) was assessed as a response parameter using STATISTIC 8.0 software, where the statistical significance between the different treatments was set at $p < 0.05$ using ANOVA.

Various simple mathematical models have been developed to predict the dynamic behavior of the column, such as Adams-Bohart, Thomas, and Dose–response. Thus, the experimental data of the breakthrough curves were fitted to the described models.

Results and discussion

Biosorbent characterization

The determination of pH$_{PZC}$ assumes that protons (H^+) and hydroxyl groups (OH^-) are the determinant ions. Thus, the adsorbent present in aqueous solution can adsorb H^+ or OH^- ions, that is, it can dissociate or associate solution protons, depending on the properties of the adsorbent and the pH of the aqueous solution. Thus, the surface of the active sites becomes positively charged when associating protons under acidic conditions or negatively charged when dissociating protons under alkaline conditions (Cerovic et al. 2007).

Figure 1 determines the pH$_{PZC}$ for MO seeds, which corresponds to the range where the final pH remains constant. For MO seeds, pH$_{PZC}$ lies at approximately 6.5, favoring the adsorption of nitrate ions at a pH below this value.

The biosorbent morphology was investigated by SEM analysis and the micrographs obtained are shown in Fig. 2 at a magnitude of 1000 times. For MO seeds, we see a relatively porous matrix with heterogeneous pore distribution also found by Meneghel et al. (2013) which can be attributed to the presence of a wide variety of components. Also, deformations are observed that can provide a highly specific internal surface area, favoring the adsorption of pollutants (Reddy et al. 2011).

Knowledge of the functional groups present in the adsorbent is important for understanding the mechanisms of adsorption, as these can act as adsorption sites (do Nascimento et al. 2014). The FTIR spectra obtained from the MO seeds before and after the biosorption process for nitrate ions are shown in Fig. 3.

The FTIR spectra is very similar to the one found by Araújo et al. (2010) and show the presence of various functional groups, indicating the complex nature of MO seeds. The extended band located at 3420 cm^{-1} before biosorption indicates the presence of hydroxyl groups present in proteins, fatty
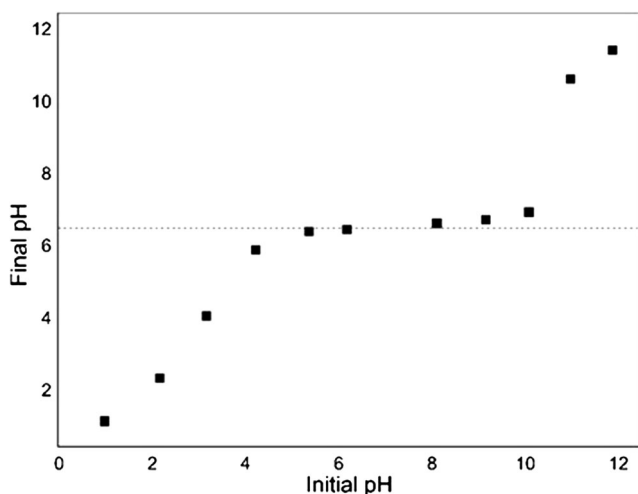
Fig. 1 Determination of pH_{PZC} for *Moringa oleifera* Lam seeds (biosorbent mass 0.05 g, pH 1–12, rotation 100 rpm, temperature 25 °C, and time 24 h)

acids, carbohydrates, phenolics, silanols, and lignin units (Reddy et al. 2011) with a slight decrease after nitrate ion biosorption. The peaks at 2923 and 2852 cm^{-1} before and after biosorption indicate the symmetric and asymmetric stretching of C–H of CH_2 groups present in fatty acids. In the region 1800–1500 cm^{-1}, a number of bands that overlap are observed which can be attributed to C=O stretching. The peak observed at 1653 cm^{-1} is related to amide groups present in proteins. The peak observed at 1587 cm^{-1} can be assigned to stretching connecting C–N and also deformation of the N–H bond present in the seed proteins (Araújo et al. 2010, 2013). By comparison between before and after the nitrate ion biosorption process, the changes observed for spectra may be due to electrostatic interactions between the functional groups present in the MO seeds, especially the amide groups present in proteins with nitrate ions.
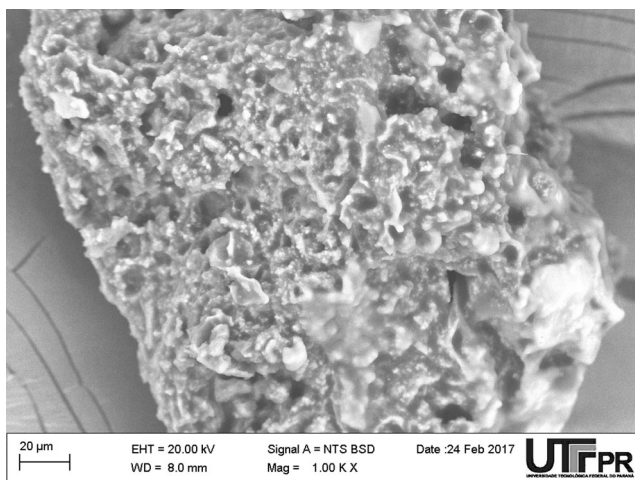
Fig. 2 Micrograph obtained by SEM of the *Moringa oleifera* Lam seeds
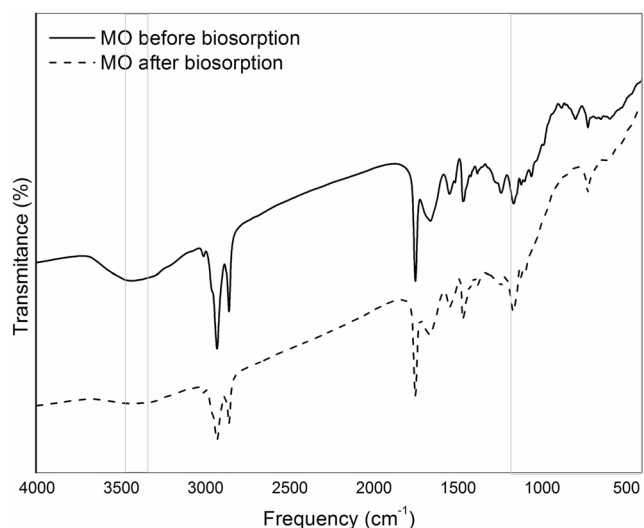
Fig. 3 FTIR spectra of *Moringa oleifera* Lam seeds before and after nitrate biosorption (biosorbent mass 0.2 g, pH 5, rotation 100 rpm, temperature 25 °C, and time 24 h)

Batch biosorption assays

Kinetic study

Figure 4 presents the adjustment of experimental data to kinetic models of (a) pseudo-first-order and pseudo-second-order models and (b) intraparticle diffusion model to equilibrium of nitrate in MO.

From Fig. 4a, it is also possible to determine the equilibrium time for this adsorption. The results for the residence time required for adsorbate equilibrium within the biosorbent pores suggest that the removal of nitrate is rapid for the first few minutes, followed by a decrease in removal until reaching equilibrium from the time of 240 min, presenting no difference for the later evaluated times. Pseudo-first-order (Lagergren 1898), pseudo-second-order (Ho and Mckay 1998), and intraparticle diffusion (Weber and Morris 1963) kinetic models (Eqs. 8, 9, and 10 respectively) were adjusted to the experimental data (Fig. 4) and the parameters of the models, as well as their correlation, are shown in Table 1.

$$q_t = q_e\left(1 - e^{-k_1 . t}\right) \qquad (8)$$

$$q_t = q_e \frac{(q_e . k_2 . t)}{(q_e . k_2 . t + 1)} \qquad (9)$$

$$q_t = k_{dif} . t^{\beta} + C \qquad (10)$$

where q_t is the nitrate amount adsorbed at t time (mg g^{-1}), q_e is the nitrate amount adsorbed at equilibrium (mg g^{-1}), t is the stirring time (min), k_1 is the constant rate of adsorption of the pseudo-first-order model (min^{-1}), k_2 is the constant rate of adsorption of the pseudo-second-order model (g mg^{-1} min^{-1}), and C (mg g^{-1}) is a constant related to diffusion
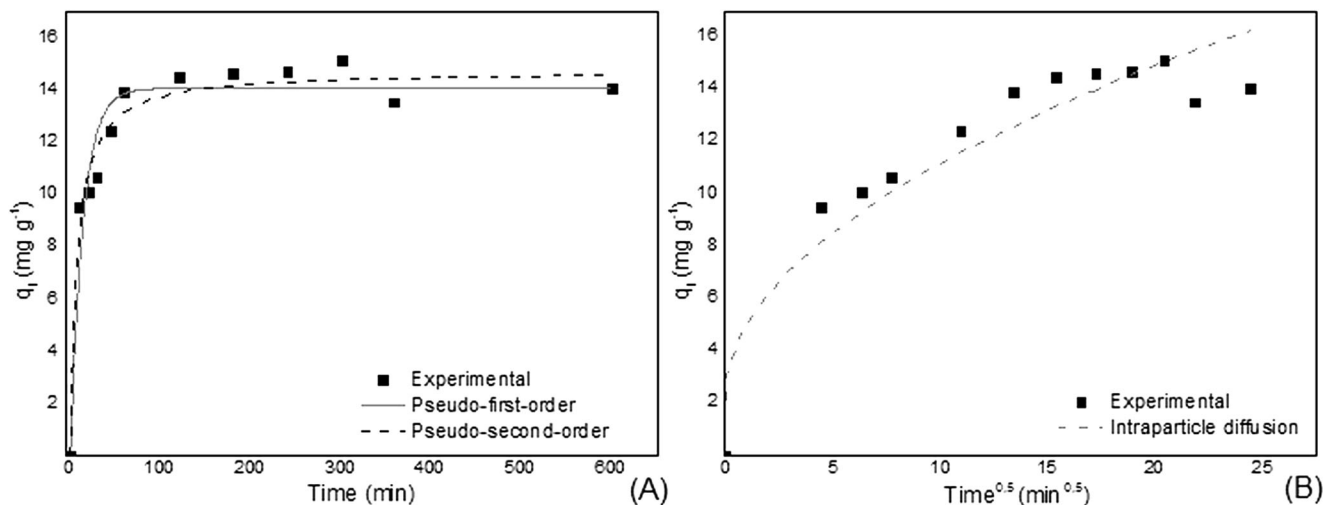
Fig. 4 Adjustment of experimental data to kinetic models of **a** pseudo-first-order and pseudo-second-order models and **b** intraparticle diffusion model (biossorbent mass 0.2 g, pH 5, rotation 100 rpm, temperature 25 °C, and contact time 10–600 min)

resistance. The value of k_{dif} (mg g^{-1} min$^{-0.5}$) may be obtained from the slope and the value of C from the intersection of the graph curve q_t versus $t^{0.5}$.

By means of Table 1, for the intraparticle diffusion model, a C value other than zero indicates that the lines of the graph (Fig. 4b) do not pass through the origin, and therefore it is not a determinative kinetics step. However, both pseudo-first-order and pseudo-second-order kinetic models presented correlations greater than 90%, and q_e values very close to the experimental values, but the pseudo-second-order model best represented the experimental data. Processes that follow this model have the characteristic of chemisorption as a limiting step (Debrassi et al. 2011), involving valence forces or exchange of electrons between adsorbate and adsorbent (Ncibi et al. 2008). Thus, the adsorbate adheres to the functional groups present on the surface of the adsorbent through chemical bonding.
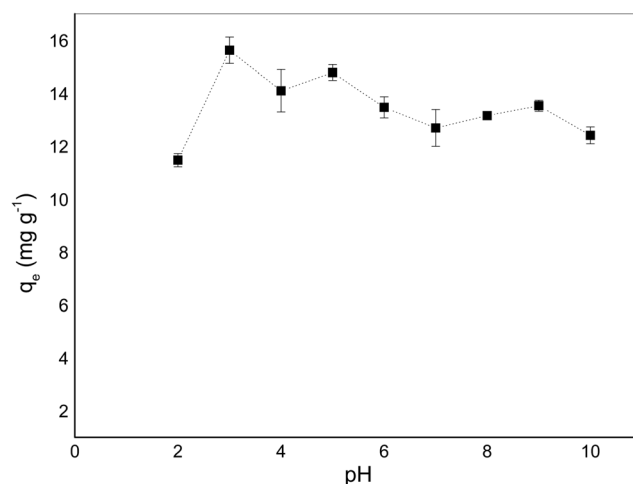
Influence of pH

The influence of pH on adsorption is important, since the loads of adsorbent and adsorbate must be opposed so that there is electrostatic interaction between them (Toledo et al. 2005). The results show that nitrate adsorption is dependent on solution pH, where ion removal is favored by acidic pH and the best pH is 3 (Fig. 5). At this pH, the maximum adsorption capacity was 15.62 ± 0.50 mg g^{-1}. In this pH range, the concentration of H_3O^+ ions increases and these interact with nitrate ions by electrostatic attraction (Demiral and Gündüzog 2010; Aghaii et al. 2013).

For the natural pH of water contaminated with nitrate (pH 5.0), the maximum adsorption capacity was 14.09 ± 0.3 mg g^{-1}.

Table 1 Constants of the pseudo-first-order, pseudo-second-order, and intraparticle diffusion models

q_e experimental (mg g^{-1})	14.68 ± 2.30	
Kinetic model	Parameters	
First-order	k_1 (L min^{-1})	0.0695
	q_e calculated (mg g^{-1})	14.19
	R^2	0.9302
Second-order	k_2 (g mg^{-1} min^{-1})	0.0087
	q_e calculated (mg g^{-1})	14.91
	R^2	0.9691
Intraparticle diffusion	k_{dif} (mg g^{-1} min$^{-0,5}$)	2.8471
	C (mg g^{-1})	2.1618
	R^2	0.8869

Fig. 5 Effect of nitrate biosorption onto MO seeds (biosorbent mass 0.2 g, pH 2–10, rotation 100 rpm, temperature 25 °C, and time 240 min)
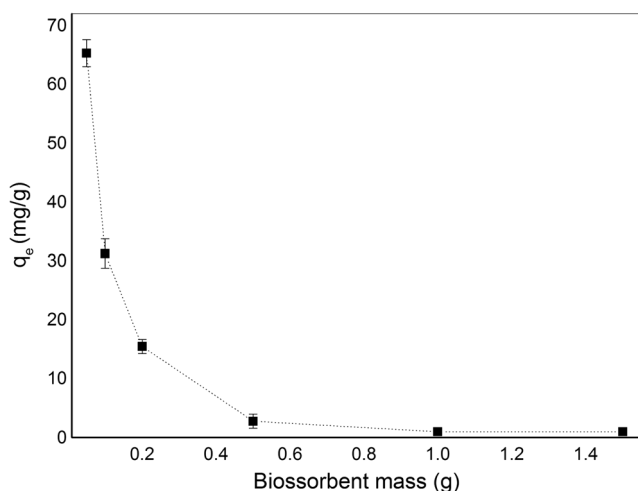
As demonstrated by the FTIR assay, MO seeds have a wide variety of functional groups, which according to Akhtar et al. (2007) can be dissociated at different pH values and, therefore, participate in the biosorption process, where different pH values can result in different nitrate removal percentages. Still, according to the pH$_{PZC}$, the best pH must be below 6.5, because from this value, the interactions get weaker. This was confirmed in the pH evaluation assay, since at pH values below 6, the highest nitrate removal capacity was obtained, except for pH 2 ($q_e = 11.46 \pm 0.25$ mg g^{-1}). Very acidic pHs, such as pH 2, may have damaged the surface of the biosorbent, a natural material.

Influence of biosorbent mass

The effect of the biosorbent mass is presented in Fig. 6. From the results, it was observed that the amount adsorbed (q_e) increases proportionately with decreasing adsorbent dosage; for MO seeds the q_e fell from 64.38 ± 2.31 mg g^{-1} with 0.05 g of bisorbent mass to 0 mg g^{-1} with 1.5 g. Thus, high q_e occurred in the use of 0.05 g of adsorbent mass, suggesting that small amounts of adsorbent are required to accommodate all of the adsorbate molecules. Moreover, MO biosorbent has a limit, from which the balance between the amount of released nitrate and that adsorbed by the seed is moved. Increasing the adsorbent mass (0.5 g or >) can harm the process, since with a greater mass of biosorbent used, the amount of nitrate released by the MO seeds increases, without removal of the ions.

Adsorption energy

The nature and thermodynamic feasibility of the nitrate adsorption process were calculated from the Gibbs free energy, enthalpy, and entropy by means of Eqs. 11, 12, and 13 wherein

the linear adjustment of the graph of *ln kd* versus *1/T* is provided to calculate $\Delta H°$ and $\Delta S°$ by its slope and intercept (Liu 2009); the results are shown in Table 2.

$$\Delta G° = -R.T.lnk_d \qquad (11)$$

$$\Delta G° = \Delta H° - T.\Delta S° \qquad (12)$$

$$\ln k_d = \frac{\Delta S°}{R} - \frac{\Delta H°}{R.T} \qquad (13)$$

It is known that for ΔH values lower than 40 kJ mol^{-1}, adsorption is described as a physical process (Bhatnagar et al. 2010; Aghaii et al. 2013). Thus, for MO, it can be concluded that physisorption takes place exothermically as evidenced by the negative values of ΔH.

These results are consistent with findings in the literature, where physical adsorption occurs by weak intermolecular forces of attraction between the surface molecules of the adsorbent and the adsorbed molecules characterized as an exothermic process, favored at low temperatures (Ruthven 1984).

In addition, the results complement what was found in the adsorption kinetics, indicating that both chemisorption and physisorption probably occur for MO seeds, despite getting a better fit of the data to the pseudo-second-order kinetic model.

The negative value of ΔS suggests reduced randomness at the solid–solution interface during the biosorption of nitrate, while negative values of ΔG suggest the spontaneous nature of the adsorption process, during the setting of nitrate ions at the active sites of the biosorbent and a favorable adsorption process for temperatures below 25 °C. According to Liu (2009): "The Gibbs energy change ($\Delta G°$) indicates the degree of spontaneity of an adsorption process, and a higher negative value reflects a more energetically favorable adsorption." Thus, the results obtained suggest that the batch adsorption process would be unspontaneous in the temperatures up to 35 °C. Other works mention that positive values of $\Delta G°$ would indicate that the adsorption process is unspontaneous under the conditions applied (Kafshgari and Tahermansouri 2017; Khakpour and Tahermansouri 2018; Yahya et al. 2018).

Fig. 6 Effect of biosorbent mass on nitrate biosorption onto MO seeds (biosorbent mass 0.05–1.5 g, pH 5, rotation 100 rpm, temperature 25 °C, and time 240 min)

Table 2 Thermodynamic parameters for the biosorption of nitrate on MO seeds at different temperatures

Thermodynamics parameters	Temperature (°C)			
	15	25	35	45
$\Delta G°$ (kJ mol^{-1})	− 0.78	− 0.22	1.14	2.45
$\Delta H°$ (kJ mol^{-1})	− 32.70			
$\Delta S°$ (kJ mol^{-1} K^{-1})	− 0.11			

$R^2 = 0.9688$

Batch desorption

Desorption assays were conducted in batches in order to check the possibility of biosorbent reuse. Regenerating agents were evaluated such as water, sodium hydroxide (pH 13), and ethanol 50% (v/v), and under the same experimental conditions, it was found that sodium hydroxide removed 95.74% of the nitrate present in the active sites of the biosorbent, while water achieved only 26.60% of removal.

Thus, this regenerative agent was used in five cycles of adsorption/desorption, where after each cycle, the biosorbent was dried and weighed.

From the results obtained, it can be concluded that the biosorption process occurs either by physisorption or chemisorption, but to a greater tendency by physisorption. That behavior was also confirmed by the adsorption/desorption test, since the regenerating agent (sodium hydroxide) was able to desorb the nitrate present at the biosorbent surface. It was observed that there was a loss of adsorptive capacity in the first two adsorption/desorption cycles, which tended to certain stability in the following biosorption cycles. This behavior can be explained by the characteristic of the natural material used in the experiment, that is, the MO seeds not undergoing chemical modifications and capable of providing structural stability. Their being a natural material, without pre-treatment, and the possibility of them working in several operating cycles, demonstrated an advantage for the use of MO seeds as a biosorbent.

Biosorption in fixed-bed column assays

Figure 7 shows the breakthrough curves obtained in the evaluation of the effect of feed concentration, pH of the initial solution, and flow rate parameters, respectively to
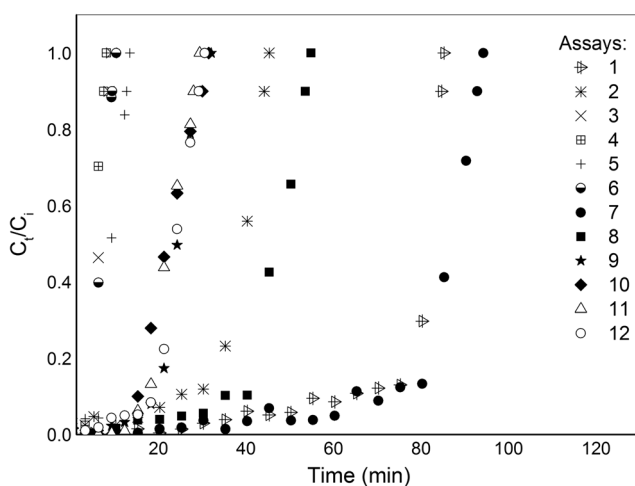
Fig. 7 Breakthrough curves for the biosorption of nitrate onto MO seeds: assays 1–12

assays 1–12. Table 3 shows the results obtained for the total capacity of the bed (q_t), maximum capacity of the bed (q_e), total amount of adsorbate sent to the bed (W_t), and total percentage removal of the bed (Y) in addition to the breakthrough (t_r) and saturation times (t_s) calculated from the breakthrough curves.

From the results, we found that the percentage of nitrate removal by biosorption ranged from 69.69 to 91.09% while the adsorptive capacity values by MO seeds (q_e) ranged from 1.59 to 7.69 mg g^{-1}.

The best experimental conditions, according to the values for percentage removal (91.09%) and maximum capacity (7.69 mg g^{-1}) of the bed were those used in assay 1, which utilized pH 3, flow rate of 1 mL min^{-1}, and initial nitrate concentration of 100 mg L^{-1}. These experimental conditions were confirmed by statistical analysis, where it was observed that the variation of pH, initial concentration, and flow rate significantly influenced the nitrate biosorption process, with a p value < 0.05.

A negative effect was obtained with pH (− 1.7546) and flow rate (− 2.0975) parameters, while a positive effect (1.6808) was obtained for initial concentration. This result indicates that lesser pH, lesser feed flow rate, and higher initial concentration will result in an increase of the maximum capacity of the bed.

The assay 6, which used experimental conditions of pH 7, flow rate of 5 mL min^{-1}, and initial concentration of 50 mg L^{-1} showed the lowest recorded values (1.59 mg g^{-1} and 69.69%). As for the pH values studied, nitrate biosorption was favored at pH values below pH$_{PZC}$, in this case 6.55, evidenced by batch biosorption assays. Thus, pH 3 explains the best experimental conditions.

The larger the difference between t_r and t_s, the larger is the unused portion of the column, which is undesirable although unavoidable. This is confirmed in assays 1, 2, 8, and 9, which were performed with the lowest flow rate. For feed flow rate, it is possible to see that the increase in flow rate from 1 to 5 mL min^{-1} caused a decrease in the saturation time. In assay 4, in only 7.22 min, and smaller difference between t_r and t_s (3.89 min), the biosorption process had reached 90% of its capacity ($C_t/C_0 = 0.9$). Christoforidis et al. (2015) reported that at high flow rates, bed saturation will occur in less time, leading to poor performance of the overall system, while at a low flow rate, the residence time in the bed will be higher, and consequently, its capacity will be higher. Gong et al. (2015) also mentions that when using high flow rate, the adsorbate may leave the packed-bed column before reaching adsorption equilibrium, because of insufficient residence time.

Under the same experimental conditions and varying the initial concentration, in assays 1 and 7, with double the initial concentration (100 mg L^{-1}) the saturation time decreased, but the amount adsorbed increased and the percentage removal was practically the same. As for saturation time, Golie and

Table 3 Results obtained in the analysis of the effect of feed concentration, initial solution pH and rate flow for the nitrate biosorption: assays 1–12

Assay	pH	Rate flow (mL min^{-1})	Initial concentration (mg L^{-1})	q_t (mg)	q_e (mg g^{-1})	W (mg)	Y (%)	t_r (min)	t_s (min)
1	3.0	1.0	100.0	7.69	7.69	8.44	91.09	63.31	84.46
2	7.0	1.0	100.0	3.64	3.64	4.38	83.00	19.55	43.86
3	3.0	5.0	100.0	3.01	3.01	4.22	71.40	3.51	8.44
4	7.0	5.0	100.0	2.53	2.53	3.61	70.14	3.33	7.22
5	3.0	5.0	50.0	2.18	2.18	3.11	70.20	6.36	12.45
6	7.0	5.0	50.0	1.59	1.59	2.28	69.69	3.74	9.14
7	3.0	1.0	50.0	4.13	4.13	4.62	89.37	71.69	92.54
8	7.0	1.0	50.0	2.24	2.24	2.66	84.26	34.79	53.24
9	5.5	3.0	75.0	5.34	5.34	6.57	81.26	19.01	29.22
10	5.5	3.0	75.0	4.85	4.85	6.69	72.56	15.41	29.74
11	5.5	3.0	75.0	5.01	5.01	6.23	80.28	16.58	27.73
12	5.5	3.0	75.0	5.23	5.23	6.81	76.78	16.38	28.91

Upadhyayula (2016) explained that at higher nitrate concentrations, the active sites of the biosorbent will be quickly filled, resulting in faster saturation. Kavianinia et al. (2012) also explained that high values for adsorption capacity are found at a higher adsorbate concentration, providing a greater driving force due to the concentration difference between the solute in the adsorbent and the solute in the solution for the transfer process overcoming the mass transfer resistance.

Mathematical modeling of the experimental data

The experimental data of the breakthrough curves were fitted to Thomas (1944), Bohart and Adams (1920), and Dose–response (Senthilkumar et al. 2006; Calero et al. 2009) models described in the literature. The Thomas model is the most general and widely used to describe the biosorption process in a fixed-bed column. This considers that the experimental data follow reversible second-order kinetics and that the reaction is controlled by mass transfer. The model also assumes a constant separation factor applicable to favorable and unfavorable isotherms (Aksu and Gönen 2004; Calero et al. 2009). The model is expressed by Eq. 14:

$$\frac{C_t}{C_0} = \frac{1}{1 + \exp\left[\left(\frac{k_{TH}}{Q}\right)(q_0 \cdot m - C_0 \cdot V_{ef})\right]} \tag{14}$$

Where C_0 is the feed concentration (mg L^{-1}), C_t is the outlet concentration (mg L^{-1}), k_{TH} is the mass transfer coefficient (mL mg^{-1} min^{-1}), q_0 is the adsorption capacity (mg g^{-1}), Q is the feed flow rate (mL min^{-1}), m is the mass of adsorbent (g), and V_{ef} is the volume of effluent sent to the column (L).

Bohart and Adams originally suggested a mathematical correlation that relates C_0/C_t and column service time (t) for

a continuous flow system. At first, the model was developed for a gas–charcoal adsorption system, but it can be applied to the quantitative description of other systems, where the adsorption rate is proportional to the residual solid capacity and the concentration of sorbed species (Kavianinia et al. 2012). However, this model is only used in the description of the initial part of the breakdown curve, that is, when $C_t/C_0 \leq 0.15$. The model is expressed by Eq. 15:

$$\frac{C_t}{C_0} = e^{k_{AB} \cdot C_0 \cdot t} - \left(k_{AB} \cdot N_0 \cdot \frac{H}{F}\right) \tag{15}$$

where C_0 is the feed concentration (mg L^{-1}), C_t is the outlet concentration (mg L^{-1}), k_{AB} is the kinetic constant (L mg^{-1} min^{-1}), t is the time (min), N_0 is the volumetric adsorption capacity of the bed (mg L^{-1}), H is the bed height (cm), and F is the linear velocity (cm min^{-1}). F may be obtained by the ratio between the volumetric flow (mL min^{-1}) and, A, the area of the column section (cm^2) (Gong et al. 2015).

The Dose–response model, commonly used in pharmacology to describe different processes, can also be used to describe the kinetics of biosorption in a fixed-bed column. The model is expressed by Eq. 16:

$$\frac{C_t}{C_0} = 1 - \frac{1}{1 + \left(\frac{C_i \cdot V_{ef}}{q_0 \cdot m}\right)^a} \tag{16}$$

where C_0 is the feed concentration (mg L^{-1}), C_t is the outlet concentration (mg L^{-1}), V_{ef} is the volume of effluent sent to the column (L), q_0 is the adsorption capacity (mg g^{-1}), m is the mass of adsorbent (g), and a the constant of the Dose–response model.

Adjustments according to Thomas, Dose–response, and Bohart and Adams models are shown in Table 4. From this, we realized that by the Bohart–Adams model, the value of the

Table 4 Parameters of the breakthrough curves fitted to Dose–response, Thomas, and Bohart–Adams models

Assays	Dose–response			Thomas			Bohart–Adams		
	q_0	a	R^2	q_0	k_{TH}	R^2	k_{AB}	N_0	R^2
1	8.11	61.05	0.9478	8.11	7.31	0.9483	0.0020	5346.77	0,9680
2	3.84	14.18	0.9611	3.85	3.52	0.9672	0.0013	2820.59	0.9926
3	3.06	8.02	0.9951	3.07	11.21	0.9963	0.0034	2789.45	0.9615
4	2.72	8.84	0.9964	2.71	14.23	0.9972	0.0036	2402.33	0.9126
5	2.24	7.05	0.9916	2.28	14.58	0.9894	0.0048	2034.51	0.9626
6	1.60	6.60	0.9956	1.63	18.27	0.9955	0.0057	1533.18	0.9454
7	4.30	26.28	0.9700	3.61	7.07	0.9719	0.0021	2945.40	0.9853
8	2.31	13.79	0.9773	2.32	5.75	0.9803	0.0022	1707.18	0.9869
9	5.40	11.26	0.9957	5.42	6.06	0.9973	0.0017	4361.68	0.9332
10	4.83	6.40	0.9930	4.91	3.97	0.9933	0.0014	4306.06	0.9391
11	4.94	8.68	0.9927	4.99	5.14	0.9932	0.0019	4048.13	0.9615
12	5.31	10.40	0.9908	5.34	5.66	0.9934	0.0019	4211.55	0.9672

kinetics constant k_{AB} increases with increasing flow rate and pH; however, it decreases with an increase of the initial concentration. The influence of the flow rate on the constant k_{AB} demonstrates that the kinetics of the system is dominated by external mass transfer, as also observed by (Aksu and Gönen 2004).

As for N_0 concern, the volumetric adsorption capacity of the bed, the Bohart and Adams model presented better fit to the data referent to assay 2. For these conditions (pH 7.0, flow rate of 1 mL min^{-1}, and concentration of 100 mg L^{-1}), the N_0 value obtained was 2820.59 mg L^{-1}.

The Dose–response model represented the experimental data well, with correlations greater than 90% and adsorptive capacity values very close to those obtained experimentally for all assays. q_0 and a increased with increasing concentration and decreasing pH and flow rate. For this model, the best settings occurred for assay 4, with correlations of $R^2 = 0.9964$ while the q_0 value (2.72 mg g^{-1}) was closest to the experimental value (2.53 mg g^{-1}). The conditions of this assay were pH 7.0, flow rate of 5 mL min^{-1}, and concentration of 100 mg L^{-1}.

Finally, the Thomas model was the one that best represented the experimental data, especially for assay 9 with adsorptive capacity value (5.42 mg g^{-1}) very close to those obtained experimentally (5.34 mg g^{-1}). q_0 and k_{TH} increased with increasing concentration, whereas for the flow rate, k_{TH} increased with increasing flow rate and q_0 had the opposite effect. Aksu and Gönen (2004) explained that the Thomas model best fits the experimental data when the process in a fixed-bed adsorption column has no limiting step such as internal or external diffusion.

Conclusions

The removal of nitrate from aqueous solutions was conducted in a batch and continuous fixed-bed column system using *Moringa oleifera* biosorbent. To the batch system, the effects like adsorbent mass, pH, and time were studied, and results showed that nitrate biosorption is enhanced under experimental conditions of pH 3 and a biosorbent mass of 0.05 g. The effects of process parameters such as flow rate, pH, and initial nitrate concentration of packed-bed on the performance of adsorption column were also investigated, and an adsorptive capacity of 7.69 mg g^{-1} was obtained at the conditions of pH 3, 1 mL min^{-1}, and 100 mg L^{-1}. Thus, MO seeds present a promising potential for nitrate removal, obtaining high adsorption capacities under optimum conditions, and it can be applied in both biosorption batch and fixed-bed column processes. It can be emphasized that one additional advantage of working with MO seeds is their desorption capacity, being able to operate in multiple cycles of operation.

References

Aghaii MD, Pakizeh M, Ahmadpour A (2013) Synthesis and characterization of modified UZM-5 as adsorbent for nitrate removal from aqueous solution. Sep Purif Technol 113:24–32. https://doi.org/10.1016/j.seppur.2013.04.013

Akhtar M, Hasany SM, Bhanger MI, Iqbal S (2007) Sorption potential of *Moringa oleifera* pods for the removal of organic pollutants from aqueous solutions. 141:546–556. https://doi.org/10.1016/j.jhazmat.2006.07.016

Aksu Z, Gönen F (2004) Biosorption of phenol by immobilized activated sludge in a continuous packed bed: prediction of breakthrough

curves. Process Biochem 39:599–613. https://doi.org/10.1016/S0032-9592(03)00132-8

Amagloh FK, Benang A (2009) Effectiveness of Moringa oleifera seed as coagulant for water purification. Afr J Agric Res 4:119–123

Araújo CST, Alves VN, Rezende HC, Almeida ILS, de Assunção RMN, Tarley CRT, Segatelli MG, Coelho NMM (2010) Characterization and use of Moringa oleifera seeds as biosorbent for removing metal ions from aqueous effluents. Water Sci Technol 62:2198–2203

Araújo CST, Carvalho DC, Rezende HC et al (2013) Bioremediation of waters contaminated with heavy metals using Moringa oleifera seeds as biosorbent. Appl Bioremediation-Active Passiv Approaches: 227–255. https://doi.org/10.5772/56157

Baptista ATA, Coldebella PF, Henrique P et al (2015) Coagulation-flocculation process with ultrafiltered saline extract of Moringa oleifera for the treatment of surface water. Chem Eng J 276:166–173. https://doi.org/10.1016/j.cej.2015.04.045

Baptista ATA, Silva MO, Gomes RG, Bergamasco R, Vieira MF, Vieira AMS (2017) Protein fractionation of seeds of Moringa oleifera Lam and its application in superficial water treatment. Sep Purif Technol 180:114–124

Bhatnagar A, Sillanpää M (2011) A review of emerging adsorbents for nitrate removal from water. Chem Eng J 168:493–504. https://doi.org/10.1016/j.cej.2011.01.103

Bhatnagar A, Kumar E, Sillanpää M (2010) Nitrate removal from water by nano-alumina: characterization and sorption studies. 163:317–323. https://doi.org/10.1016/j.cej.2010.08.008

Bohart GS, Adams EQ (1920) Some aspects of the behavior of charcoal with respect to chlorine. J Frankl Inst 42:523–544

Calero M, Hernáinz F, Blázquez G, Tenorio G (2009) Study of Cr (III) biosorption in a fixed-bed column. J Hazard Mater 171:886–893. https://doi.org/10.1016/j.jhazmat.2009.06.082

Cerovic LS, Milonjic SK, Todorovic MB et al (2007) Point of zero charge of different carbides. Colloids Surf A Physicochem Eng Asp 297:1–6. https://doi.org/10.1016/j.colsurfa.2006.10.012

Christoforidis AK, Orfanidis S, Papageorgiou SK, Lazaridou AN, Favvas EP, Mitropoulos AC (2015) Study of Cu (II) removal by Cystoseira crinitophylla biomass in batch and continuous flow biosorption. Chem Eng J 277:334–340. https://doi.org/10.1016/j.cej.2015.04.138

Debrassi A, Claudia M, Largura T et al (2011) Adsorção do corante vermelho congo por derivados da O-Carboximetilquitosana hidrofobicamente modificados. Quim Nova 34:764–770

Demiral H, Gündüzog G (2010) Removal of nitrate from aqueous solutions by activated carbon prepared from sugar beet bagasse. Bioresour Technol 101:1675–1680. https://doi.org/10.1016/j.biortech.2009.09.087

do Nascimento RF, Lima ACA d, Vidal CB et al (2014) Adsorção: aspectos teóricos e aplicações ambientais. Imprensa Universitária, Fortaleza

Eneji AE, Islam R, An P, Amalu UC (2013) Nitrate retention and physiological adjustment of maize to soil amendment with superabsorbent polymers. J Clean Prod 52:474–480. https://doi.org/10.1016/j.jclepro.2013.02.027

Farrokhzadeh H, Ebrahimi A, Taheri E, Dastjerdi MV (2013) Effectiveness of moringa oleifera powder in removal of heavy metals from aqueous solutions. Fresenius Environ Bull 22:1516–1523

Galloway JN, Aber JD, Erisman JW et al (2003) The nitrogen cascade. Am Inst Biol Sci 53:341–356

Golie WM, Upadhyayula S (2016) Continuous fixed-bed column study for the removal of nitrate from water using chitosan/alumina composite. J Water Process Eng 12:58–65

Gong J, Zhang Y, Jiang Y et al (2015) Applied surface science continuous adsorption of Pb(II) and methylene blue by engineered graphite oxide coated sand in fixed-bed column. Appl Surf Sci 330:148–157. https://doi.org/10.1016/j.apsusc.2014.11.068

Gopalakrishnan L, Doriya K, Kumar DS (2016) Moringa oleifera: a review on nutritive importance and its medicinal application. Food Sci Human Wellness 5:49–56

Ho YS, Mckay G (1998) Kinetic models for the sorption of dye from aqueous solution by wood. Process Saf Environ Prot 76:183–191

IAL (2008) Águas. In: Métodos físico-químicos para análise de alimentos, 4th edn. Instituto Adolfo Lutz, São Paulo, pp 366–367

Jain S, Bansiwal A, Biniwale RB, Milmille S, Das S, Tiwari S, Siluvai Antony P (2015) Enhancing adsorption of nitrate using metal impregnated alumina. Biochem Pharmacol 3:2342–2349. https://doi.org/10.1016/j.jece.2015.08.009

Kafshgari MM, Tahermansouri H (2017) Development of a graphene oxide/chitosan nanocomposite for the removal of picric acid from aqueous solutions: Study of sorption parameters. Colloids Surf B: Biointerfaces 160:671–681. https://doi.org/10.1016/j.colsurfb.2017.10.019

Kavrianinia I, Plieger PG, Kandile NG, Harding DRK (2012) Fixed-bed column studies on a modified chitosan hydrogel for detoxification of aqueous solutions from copper (II). Carbohydr Polym 90:875–886. https://doi.org/10.1016/j.carbpol.2012.06.014

Khakpour R, Tahermansouri H (2018) Synthesis, characterization and study of sorption parameters of multi-walled carbon nanotubes/chitosan nanocomposite for the removal of picric acid from aqueous solutions. Int J Biol Macromol 109:598–610. https://doi.org/10.1016/j.ijbiomac.2017.12.105

Lagergren S (1898) Zur theorie der sogenannten adsorption gelösterstoffe. Bihang TillKungligaSvenskaVetenskaps-akademiens. Handlingar 24: 1–39

Liu Y (2009) Is the free energy change of adsorption correctly calculated? J Chem Eng 54:1981–1985

Matouq M, Jildeh N, Qtaishat M, Hindiyeh M, al Syouf MQ (2015) The adsorption kinetics and modeling for heavy metals removal from wastewater by Moringa pods. J Environ Chem Eng 3:775–784. https://doi.org/10.1016/j.jece.2015.03.027

Meneghel AP, Celso A, Jr G et al (2013) Biosorption of cadmium from water using Moringa (Moringa oleifera Lam .) seeds. Water Air Soil Pollut 224:1383–1396. https://doi.org/10.1007/s11270-012-1383-2

Ncibi MC, Mahjoub B, Seffen M (2008) Investigation of the sorption mechanisms of metal-complexed dye onto Posidonia oceanica (L .) fibres through kinetic modelling analysis. Bioresour Technol 99: 5582–5589. https://doi.org/10.1016/j.biortech.2007.10.040

Nguyen TAH, Ngo HH, Guo WS, Pham TQ, Li FM, Nguyen TV, Bui XT (2015) Adsorption of phosphate from aqueous solutions and sewage using zirconium loaded okara (ZLO): fixed-bed column study. Sci Total Environ J 523:40–49. https://doi.org/10.1016/j.scitotenv.2015.03.126

Ota K, Amano Y, Aikawa M, Machida M (2013) Removal of nitrate ions from water by activated carbons (ACs)—influence of surface chemistry of ACs and coexisting chloride and sulfate ions. Appl Surf Sci 276:838–842. https://doi.org/10.1016/j.apsusc.2013.03.053

Paudyal H, Pangeni B, Inoue K, Kawakita H, Ohto K, Alam S (2013) Adsorptive removal of fluoride from aqueous medium using a fixed bed column packed with Zr(IV) loaded dried orange juice residue. Bioresour Technol 146:713–720. https://doi.org/10.1016/j.biortech.2013.07.014

Reddy DHK, Ramana DKV, Seshaiah K, Reddy AVR (2011) Biosorption of Ni(II) from aqueous phase by Moringa oleifera bark , a low cost biosorbent. Desalination 268:150–157. https://doi.org/10.1016/j.desal.2010.10.011

Regalbuto JR, Robles JO (2004) The engineering of Pt/carbon catalyst preparation for application on proton exchange fuel cell membrane (PEFCM). Catalysis Laboratory University of Illinois at Chicago Progress Report, Chicago

Rezende D, Nishi L, Coldebella PF, Silva MF, Vieira MF, Vieira AMS, Bergamasco R, Fagundes-Klen MR (2016) Groundwater nitrate contamination: assessment and treatment using Moringa oleifera

Lam. seed extract and activated carbon filtration. Can J Chem Eng 94:725–732

Ruthven DM (1984) Principles of adsorption and adsorption processes. John Wiley & Sons, New York

Senthilkumar R, Vijayaraghavan K, Thilakavathi M et al (2006) Seaweeds for the remediation of wastewaters contaminated with zinc (II) ions. J Hazard Mater 136:791–799. https://doi.org/10.1016/j.jhazmat.2006.01.014

Shanmugaprakash M, Sivakumar V (2015) Batch and fixed-bed column studies for biosorption of Zn(II) ions onto pongamia oil cake (Pongamia pinnata) from biodiesel oil extraction. J Environ Manag 164:161–170

Thomas HC (1944) Heterogeneous ion exchange in a flowing system. J Am Chem Soc 66:1664–1666

Toledo IB, Ferro-Garcia MA, Rivera-Utrilla J et al (2005) Bisphenol A removal from water by activated carbon. Effects of carbon characteristics and solution chemistry. Environ Sci Technol 39:6246–6250

Weber WJ, Morris JC (1963) Kinetics of adsorption carbon from solutions. J Sanit Engeering Div Proc 89:31–60

Weyer PJ, Cerhan JR, Kross BC et al (2001) Municipal drinking water nitrate level and cancer risk in older women: the Iowa Women's Health Study. Epidemiology 11:327–338

WHO (2011) Guidelines for drinking-water quality. WHO, Geneva

Yahya NY, Ngadi N, Wong S, Hassan O (2018) Transesterification of used cooking oil (UCO) catalyzed by mesoporous calcium titanate: kinetic and thermodynamic studies. Energy Convers Manag 164:210–218. https://doi.org/10.1016/j.enconman.2018.03.011

Zach-Maor A, Semiat R, Shemer H (2011) Fixed bed phosphate adsorption by immobilized nano-magnetite matrix: experimental and a new modeling approach. Adsorption 17:929–936. https://doi.org/10.1007/s10450-011-9371-1